In defense of Milankovitch: auxiliary materials

Gerard Roe

Department of Earth and Space Sciences, University of Washington, Box 351310, Seattle, WA, USA

Details of data analysis

All analyses were performed on a common timescale with equal increments of 1000 years. Where necessary, linear interpolation was used to place data onto this time scale. Second-order accurate centred-differences were used to calculate derivatives. All correlations and cross-spectra were calculated after the data had been linearly de-trended and normalized. No additional filtering was used. It has been suggested that the original SPECMAP chronology is too old by an average of 1500 yr [e.g., *Ruddiman and Raymo*, 2003]. In that case, all SPECMAP phase lags reported here would be shifted by approximately that much. The interpretation of the results presented would be unaffected.

To evaluate the sensitivity of the results to the method, first-, second-, and third- order accurate differencing schemes were tested, as well as cubic-spline and nearest-neighbour interpolation. None of these changes affected the results.

Cross-spectral analysis of relationship between insolation and dV/dt

Fig. S1 shows an estimate of cross-spectral coherence and phase between *dV/dt* and June 65N insolation for the two different ice volume reconstructions. Both records show significant coherence between the insolation and *dV/dt* at orbital frequencies (obliquity ~2.5 cycles per 100~kyr, climatic precession ~4.3 & 5.3 cycles per 100 kyr). The cross-spectral phase over this range is consistent with the lag-correlation analysis indicating a direct and essentially anti-phased relationship between high latitude insolation and *dV/dt.* A relatively large bandwidth was used to ensure stable spectral estimates. Calculations using narrower bandwidths always show strong coherency and an anti-phased relationship at the obliquity frequency for both records, and also at the climate precession frequencies for the SPECMAP record (orbitally-tuned). For the HW04 record the coherence at the climatic precession frequencies is somewhat less stable and for some bandwidths can fall below the 95% confidence estimate indicated by the dashed line in Fig. A1. The larger bandwidth used here is justified by the expectation that the non-linear diffusive nature of ice dynamics will lead to a broad-band spectral response of the ice sheet to the narrow-band insolation forcing [e.g., *Pollard*, 1982]. Note that cross-spectra of ice volume and insolation have the same coherence as displayed in Fig. A1 but show a roughly 90^o phase lag of the volume behind insolation variations.

Details of regression analyses

Linear combinations of climatic precession, ψ, and obliquity, ε, indices were regressed onto the SPECMAP and HW04 records of *dV/dt*, using the following regression model:

$$\frac{dV}{dt}(t) = \beta_1\psi(t-\tau_1) + \beta_2\varepsilon(t-\tau_2) + AR1(t),$$

where β_1, β_2 are coefficients and τ_1, τ_2 are lags that are allowed to vary. *AR1(t)* is a first order autoregressive process for the model residuals, which is used to account for auto correlations in the data in a self-consistent manner [*von Storch and Zwiers*, 1999; *Schneider and Neuman*, 2001]. The model parameters are optimized using Aikaike's final prediction error [e.g., *Schneider and Neuman*, 2001]. This optimization criterion seeks the best-fit regression model by minimizing the unexplained residuals, taking into account the number of fitting parameters used in the regression model.

Comparison of *dV/dt* with atmospheric CO_2.

Records of atmospheric CO_2 have been recovered from bubbles trapped in Antarctic ice cores. The Vostok and EPICA ice cores [*Petit et al.*, 1999; *Siegenthaler et al.*, 2005] together cover the last 650 kyr. Several different age scales have been suggested for the Vostok ice core, based on different assumptions [*Petit et al.*, 1999; *Ruddiman and Raymo*, 2003; *Shackleton*, 2000]. A ~650 kyr long record of CO_2 was created using the RR03 age scale for Vostok [*Ruddiman and Raymo*, 2003] (between 397 ka and 10 ka) and the published age scale for EPICA [*Siegenthaler et al.*, 2005] (between 649 ka and 397 ka). Lag correlation analyses were performed to establish the relationship between CO_2 and *dV/dt* (Fig. A2). For the SPECMAP record the maximum correlation of -0.35 is obtained when *dV/dt* leads CO_2 by 3 kyr, suggesting CO_2 responds to, rather than being the driving cause of, changes in ice volume. For the HW04 record the maximum correlation of -0.25, is obtained when *dV/dt* leads CO_2 by 4 kyr.

To evaluate the robustness of the relationship between CO_2 and *dV/dt*, the analysis was repeated for each of the Vostok time scales mentioned above over both the full 650 kyr period, and also over the shorter 400 kyr period covering just the Vostok record, using both SPECMAP and HW04 ice volume reconstructions. The results are summarized in Table A1. A lag of CO_2 variations behind *dV/dt* is indicated in all instances, except for the 397 ka to 10 ka (i.e., Vostok only) interval, when using HW04 record with either the RR03 [*Ruddiman and Raymo*, 2003] or SH00 [*Shackleton*, 2000] age scales, when zero lag is indicated, making the causal relationship between the two less clear-cut. However, cross-spectral analyses indicate that, even in these cases, CO_2 variations lag *dV/dt* at orbital frequencies.

Auxiliary material bibliography

Schneider, T., and A. Neumaier (2001), Algorithm 808: ARFIT—A Matlab package for the estimation of parameters and eigenmodes of multivariate autoregressive models. *ACM Trans. Math. Software* **27,** 58–65.

Petit, J.R. *et al.* (1999), Climate and atmospheric history of the past 420,000 years from the Vostok ice core, Antarctica. *Nature*, **399**, 429-436.

Pollard, D. (1982), A simple ice sheet model yields realistic 100 kyr glacial cycles. *Nature*, **296**, 334-338.

Ruddiman, W. F., and M. E. Raymo (2003), A methane based time scale for Vostok ice. *Quat. Sci. Rev.* **22**, 141-155.

Shackleton, N.J. (2000), The 100,000-year ice-age cycle identified and found to lag temperature, carbon dioxide, and orbital eccentricity. *Science*, **289**, 1897-1902.

Siegenthaler, U., *et al.* (2005), Stable carbon cycle-climate relationship during the late Pleistocene. *Science*, **310**, 1313-1317.

von Storch, H., and F. W. Zwiers (1999), *Statistical Analysis in Climate Research*. Cambridge University Press, 484 pp.

Table A1.

Time period	Ice volume record	CO_2 record (and age model)	Optimum correlation	Optimal lag of CO_2 behind dV/dt
-649 ka to -10 ka	SPECMAP	Vostok (RR03) & EPICA	-0.35	3000 yrs
-649 ka to -10 ka	SPECMAP	Vostok (SH00) & EPICA	-0.33	8000 yrs
-649 ka to -10 ka	SPECMAP	Vostok (PT99) & EPICA	-0.32	8000 yrs
-649 ka to -10 ka	HW04	Vostok (RR03) & EPICA	-0.25	4000 yrs
-649 ka to -10 ka	HW04	Vostok (SH00) & EPICA	-0.30	7000 yrs
-649 ka to -10 ka	HW04	Vostok (PT99) & EPICA	-0.31	9000 yrs
-397 ka to -10 ka	SPECMAP	Vostok (RR03)	-0.47	2000 yrs
-397 ka to -10 ka	SPECMAP	Vostok (SH00)	-0.37	2000 yrs
-397 ka to -10 ka	SPECMAP	Vostok (PT99)	-0.35	9000 yrs
-397 ka to -10 ka	HW04	Vostok (RR03)	-0.31	0 yrs
-397 ka to -10 ka	HW04	Vostok (SH00)	-0.34	0 yrs
-397 ka to -10 ka	HW04	Vostok (PT99)	-0.33	8000 yrs

Table A1: Correlation analysis of the relationship between CO_2 and *dV/dt* for different age models (RR03 [Ruddiman and Raymo, 2003], SH00 [Shackleton, 2000], PT99 [Petit et al., 1999]) and ice volume reconstructions. The full interval (649 ka to 10 ka) uses both the EPICA and Vostok CO2 records. The shorter interval (397 ka to 10 ka) uses only the Vostok record, for which the age control is better. Cross spectra for all the combinations shown above indicate CO_2 variations lag *dV/dt* at orbital frequencies.

Auxiliary material figures

Figure A1. Cross-spectral coherence and phase estimates between (-1 × June 65N insolation) and the SPECMAP (panels a and c) and the HW04 (panels b and d) reconstructions of global ice volume for the last 750 kyr. A positive phase implies insolation variations lead *dV/dt*. The vertical bars denote the frequencies of the obliquity (2.5 cycles per 100 kyr), and climatic precession (4.3 and 5.3 cycles per 100 kyr). Shaded regions indicate approximate 95% confidence bounds on the phase. A periodogram estimate using a Hanning window with 20 degrees of freedom was used. 95% confidence estimates on the coherence (dashed line) and coherence and bandwidth ranges (blue cross) are shown in panels a and b. In panels c and d, the grey shaded region gives the 95% confidence estimates for the phase range. At higher frequencies the absence of coherence together with a noisy phase relationship suggests no connection between the records there, nor would one be expected.

Figure A2. Comparison of atmospheric CO_2 and the time rate of change of global ice volume (*dV/dt*), over the last 650 kyr. The SPECMAP *dV/dt* is plotted leading CO_2 by 3 kyr, which gives the maximum lag correlation of -0.35. The HW04 *dV/dt* is shown leading CO_2 by 4 kyr, which gives the maximum lag correlation also of -0.25. Note the reversed axis for atmospheric CO_2. To clarify the presentation, the *dV/dt* curves have been rescaled, and for the comparison with the HW04 record, the CO_2 curve has repeated and offset on the y-axis.

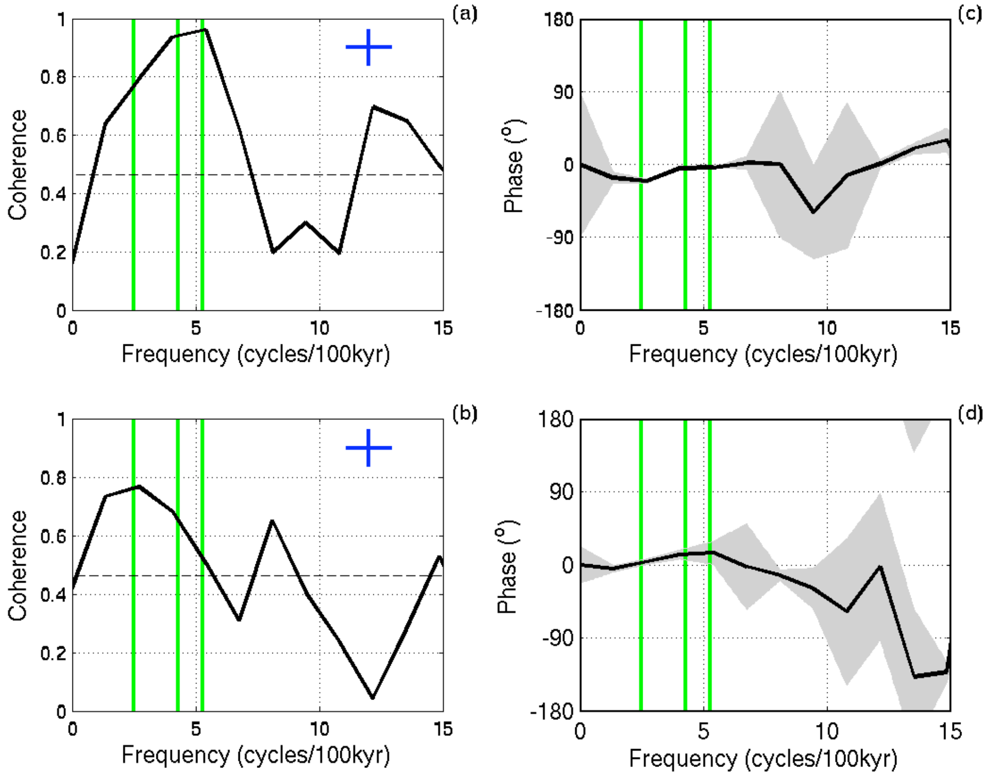

Figure A1. Cross-spectral coherence and phase estimates between (-1 × June 65N insolation) and the SPECMAP (panels a and c) and the HW04 (panels b and d) reconstructions of global ice volume for the last 750 kyr. A positive phase implies insolation variations lead *dV/dt*. The vertical bars denote the frequencies of the obliquity (2.5 cycles per 100 kyr), and climatic precession (4.3 and 5.3 cycles per 100 kyr). Shaded regions indicate approximate 95% confidence bounds on the phase. A periodogram estimate using a Hanning window with 20 degrees of freedom was used. 95% confidence estimates on the coherence (dashed line) and coherence and bandwidth ranges (blue cross) are shown in panels a and b. In panels c and d, the grey shaded region gives the 95% confidence estimates for the phase range. At higher frequencies the absence of coherence together with a noisy phase relationship suggests no connection between the records there, nor would one be expected.

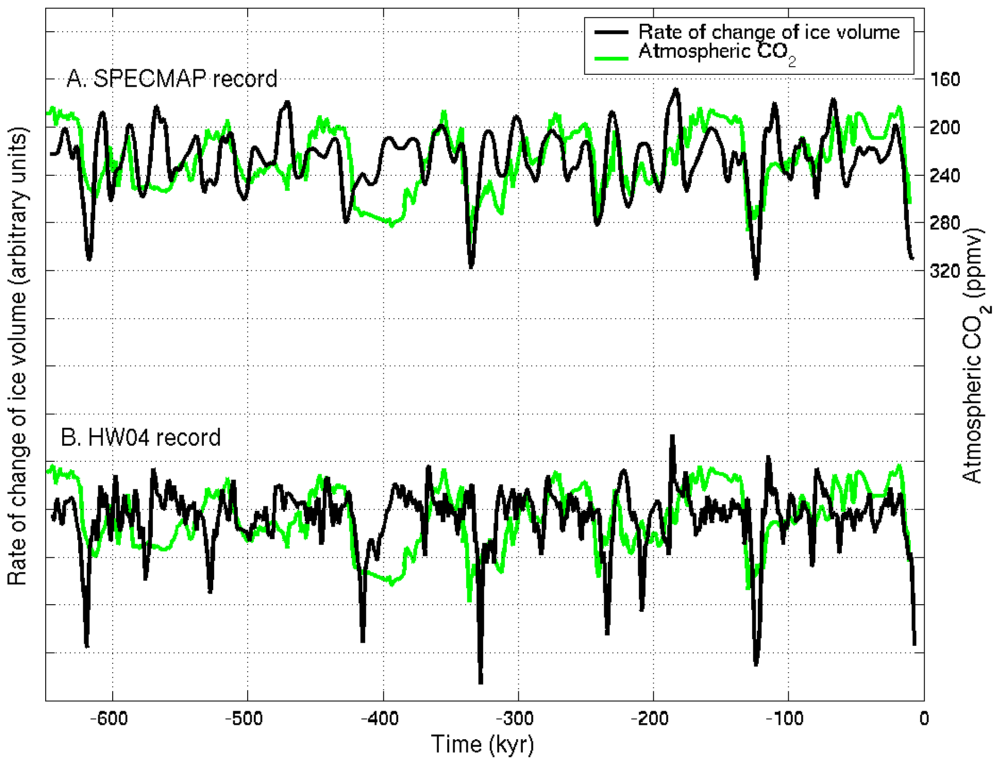

Figure A2. Comparison of atmospheric CO_2 and the time rate of change of global ice volume (*dV/dt*), over the last 650 kyr. The SPECMAP *dV/dt* is plotted leading CO_2 by 3 kyr, which gives the maximum lag correlation of -0.35. The HW04 *dV/dt* is shown leading CO_2 by 4 kyr, which gives the maximum lag correlation also of -0.25. Note the reversed axis for atmospheric CO_2. To clarify the presentation, the *dV/dt* curves have been rescaled, and for the comparison with the HW04 record, the CO_2 curve has repeated and offset on the y-axis.